

Tschörtnerite, a copper-bearing zeolite from the Bellberg volcano, Eifel, Germany

H. EFFENBERGER,¹ G. GIESTER,¹ W. KRAUSE,² AND H.-J. BERNHARDT³

¹Institut für Mineralogie und Kristallographie, Universität Wien, Althanstrasse 14, A-1090 Vienna, Austria

²Henriette-Lott-Weg 8, D-50354 Hürth, Germany

³Ruhr-Universität Bochum, Institut für Mineralogie, Universitätsstrasse 150, D-44780 Bochum, Germany

ABSTRACT

The new mineral tschörtnerite, ideally $\text{Ca}_4(\text{K,Ca,Sr,Ba})_3\text{Cu}_3(\text{OH})_8[\text{Si}_{12}\text{Al}_{12}\text{O}_{48}] \cdot x\text{H}_2\text{O}$, $x \geq 20$, occurs as well-formed cubes up to a maximum size of 0.15 mm in a Ca-rich xenolith at the Bellberg volcano near Mayen, Eifel, Germany. The light blue, transparent crystals are optically isotropic, $n = 1.504(2)$. Microprobe analysis (in weight percent) gave CaO 13.10, CuO 9.64, SrO 4.49, BaO 1.93, K_2O 1.37, Fe_2O_3 0.30, Al_2O_3 25.21, SiO_2 30.25, H_2O (calc. by difference) 13.71. The empirical formula based on 48 O atoms within the tetrahedral net is $\text{Ca}_{5.60}\text{Sr}_{1.04}\text{K}_{0.70}\text{Ba}_{0.30}\text{Cu}_{2.90}\text{Fe}_{0.09}\text{Al}_{11.85}\text{Si}_{12.06}\text{O}_{48}(\text{OH})_{8.44} \cdot 14.01\text{H}_2\text{O}$. Tschörtnerite is cubic, space group $Fm\bar{3}m$ [$a = 31.62(1)$ Å, $V = 31614$ Å³, $Z = 16$]. The density is $D_{\text{meas}} = 2.1$ g/cm³, $D_{\text{calc}} = 2.10$ g/cm³. Single-crystal X-ray investigations showed that tschörtnerite is a zeolite; the structure contains interconnection of double six-rings, double eight-rings, sodalite cages, truncated cubo-octahedra, and previously unknown 96-membered cages (tschörtnerite cage). A new structural unit is the $[\text{Cu}_{12}(\text{OH})_{24}]\text{Ca}_8\text{O}_{24}(\text{H}_2\text{O})_8$ cluster centered within the truncated cubo-octahedron. The cluster is formed by a rhombododecahedron-like arrangement of corner connected CuO_4 squares, the eight CaO_7 polyhedra are branched. The sodalite cage houses $\text{Ca}_4(\text{OH})_4\text{O}_{12}$ clusters of edge-sharing CaO_6 octahedra. Half-occupied (K,Ca,Sr,Ba) positions were located in the basal and top face of the double eight-rings, i.e., the border to the tschörtnerite cage. Within the large tschörtnerite cage only H_2O molecules were localized.

INTRODUCTION

In 1993, very small light-blue crystals were detected in one xenolith of the Bellberg volcano, Eifel, Germany. The crystals turned out to be a new zeolite mineral with some remarkable structural features: (1) a conspicuously large unit cell; larger cells have been described for the zeolites paulingite (Bieniok et al. 1996; Lengauer et al. 1994, 1997), NaZ-21 (Shepelev et al. 1983), and N (Fälth and Andersson 1982); (2) a topologically new and extremely large cage resulting in the lowest framework density known for a zeolite with fully cross-linked frameworks (Meier et al. 1996); (3) an ordered copper-cluster. Up to now, the incorporation of Cu into a zeolite has been described predominantly for exchange reactions (Gallezot et al. 1972; Maxwell and Boer 1975; Martí et al. 1976; Pluth et al. 1977; Lee and Seff 1981; Kaushik and Ravindranathan 1992; Vlessidis et al. 1993; Lee and Kevan 1994; Moretti 1994; Kucherov et al. 1995a, 1995b and references therein; for Cu atoms on framework sites in a pollucite analogue cf. Heinrich and Baerlocher 1991). (4) A substantial part of the non-framework cations is located on fully occupied atomic positions; they are strongly bound to the tetrahedral net, hydroxyl groups complete their regular coordination, and they show only weak interactions toward H_2O molecules. For a preliminary note see Krause et al. (1997).

The new mineral was named tschörtnerite; the name is for Jochen Tschörtner, mineral collector and finder of the new mineral, and was approved by the IMA-Commission on New Minerals and Mineral Names (no. 95-051) prior to publication. Type material including the crystal used for the structure investigation is deposited at the Institut für Mineralogie, Ruhr-Universität Bochum, Germany.

OCCURRENCE AND PARAGENESIS

Tschörtnerite occurs in the fragments of one Ca-rich xenolith in leucite tephrite lava at the Bellberg volcano (or Bellerberg on older maps), near Mayen, in the Laacher See volcano area, Eifel, Germany. The xenolith was broken into several small specimens, some containing a few crystals or even only one single crystal of the new mineral. The total amount of pure material is much below 1 mg. No further samples have been discovered. Tschörtnerite is associated with chalcopryrite, which seems to be the Cu source for the formation of the new mineral. Sometimes tschörtnerite is directly grown on altered chalcopryrite. The second copper-bearing mineral of this paragenesis is cuprite, forming octahedra sometimes grown on wollastonite needles. Tschörtnerite occurs together with other zeolites; associated species (in order of decreasing frequency) are willhendersonite, phillipsite, gismondine, strätlingite, and bellbergite.

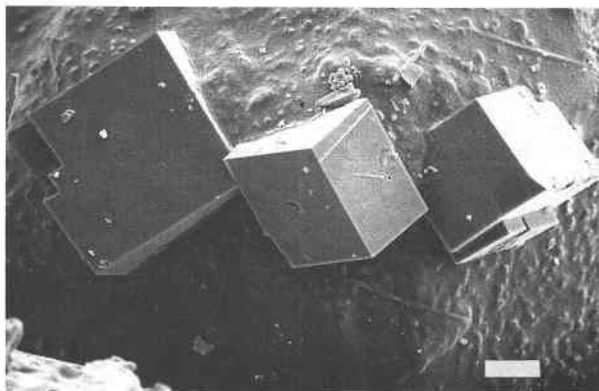


FIGURE 1. Scanning electron micrograph of tschörtnerite. The scale bar is 20 μm .

The geology, petrology, and mineralogy of the Bellberg area were discussed by Frechen (1971), Hentschel (1987), and Schüller (1990). The Bellberg volcano is well known for Ca-rich xenoliths containing rare Ca-bearing minerals. It is the type locality for ettringite (Lehmann 1874; Macleod and Hall 1991), mayenite and brownmillerite (Hentschel 1964; Colville and Geller 1971, 1972), strätlingite (Hentschel and Kuzel 1976; Rinaldi et al. 1990), eifelite (Abraham et al. 1983), reinhardbraunsite (Hamm and Hentschel 1983), jasmundite (Hentschel et al. 1983), and bellbergite (Rüdinger et al. 1993). These minerals have Ca mostly as an essential component and form silicates, sulfates, or oxides. The only exception is the K-Na-Mg silicate eifelite, which belongs to the osmilite group.

CRYSTAL PROPERTIES AND CHEMICAL COMPOSITION

Tschörtnerite usually occurs as isolated well-formed cubic crystals (Fig. 1), more rarely as parallel intergrowths. The only crystallographic form is the hexahedron {100}; no twinning was observed. The crystals are light blue, transparent, and show a vitreous luster. Tschörtnerite is optically isotropic with $n = 1.504(2)$ ($\lambda = 589$ nm). The investigated crystal showed a distinct zoning. No fluorescence was detected in either long- or short-wave ultraviolet radiation. The fracture is conchoidal, and no distinct cleavage was observed. The Vickers microhardness is 350(30) kg/mm² (measured with a Leitz microhardness tester), which corresponds to 4½ on the Mohs scale. The density of 2.1(1) g/cm³ was measured by flotation in heavy liquids. The calculated density is 2.10 g/cm³ for the composition determined by the electron-microprobe investigation. Considering the higher H₂O content indicated by the crystal-structure analysis (20 H₂O vs. 14 H₂O as derived by the microprobe analyses) the calculated density is 2.10 g/cm³. A quantitative determination of H₂O/OH was not possible because of the small amount of material available. H₂O is indicated in an infrared spectrum (Fig. 2) of a small crystal fragment using a Fourier-transform IR spectrometer and microscope. Multiple absorption bands found

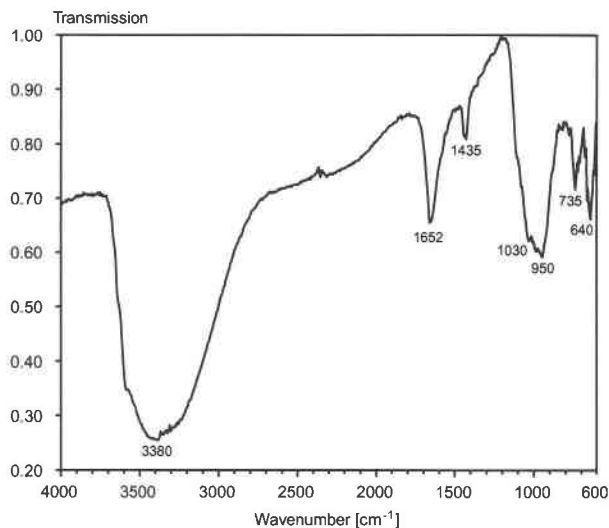


FIGURE 2. Fourier transform infrared spectrum of tschörtnerite.

from 3100 to 3600 cm⁻¹ result probably from the O-H stretching modes of the two OH groups and the individual H₂O molecules; the absorption band at 1652 cm⁻¹ is assigned to the H₂O bending mode.

Two sets of chemical analyses were carried out by electron microprobe investigations (Table 1). No other elements with atomic numbers greater than eight were detected (detection level ~0.2 wt%). H₂O was calculated by difference and its amount was taken into account during the correction procedure of the microprobe data (correction program PAP: Cameca). The lower H₂O content indicated by the microprobe analyses as compared to results of the structure determination seems to be caused by H₂O losses due to the high-vacuum measuring conditions. A part of the total amount of H₂O is given as OH in order to achieve charge balance. The calculated 8.44 OH are in reasonable agreement with the 8 OH derived from the crystal-structure determination. The uncertainty of the total amount of H₂O was

TABLE 1. Electron microprobe investigations of tschörtnerite (in wt%)

Oxide	Mean*	Range	Calculated
CaO	13.10	12.49–13.96	12.38
CuO	9.64	8.91–10.90	10.14
SrO	4.49	3.97–5.12	3.96
BaO	1.93	1.28–2.70	1.95
K ₂ O	1.37	0.79–1.66	1.20
Fe ₂ O ₃	0.30	0.13–0.61	0.00
Al ₂ O ₃	25.21	24.10–26.38	25.98
SiO ₂	30.25	29.22–31.22	30.62
H ₂ O (calc.)†	13.71		13.77
Total	100.00		100.00

Note: Cameca CAMEBAX: 15 kV, 5 nA, defocused beam (11 μm); counting time: 20 s; standards: CuSrSi₄O₁₀ (Cu,Sr), andradite (Fe,Ca), Ba glass (Ba), K glass (K), and pyrope (Al,Si).

* Mean of 13 analyses.

† Calculated for the simplified formula with 14 H₂O and assuming a K:Ca:Sr:Ba ratio 0.6:1.2:0.9:0.3 for the (K,Ca,Sr,Ba) position.

TABLE 2. Results of single-crystal X-ray data collection and structure refinements of tschörtnerite at room temperature

	STOE AED2*	NONIUS†
Detector	conventional scintillation	CCD
Range of data collection	6° < 2θ < 50°	5° < 2θ < 52.8°
Total measured reflections	10073	total rotation in φ: 360°
Observed unique reflections	1454	1955
Reflections with $F_o > 4\sigma(F_o)$	383	1769
R1 for observed; $F_o > 4\sigma(F_o)$ data	0.37; 0.15	0.065; 0.060
wR2 for unique data	0.54	0.156
w	$1/[\sigma^2(F_o^2) + (0.3278 \cdot P)^2]$	$1/[\sigma^2(F_o^2) + 0.010100 \cdot P^2]$
	$P = (\text{Max}[F_o, 0] + 2 \cdot F_o^2)/3$	$P = (\text{Max}[F_o, 0] + 2 \cdot F_o^2)/3$
Variable parameters	51	129
Max Δ/σ	≤ 0.001	≤ 0.001
Displacement parameters	isotropic (all atoms)	isotropic (H ₂ O oxygen atoms) anisotropic (all other atoms)
Final difference Fourier map	-1.67 to +3.67 e Å ⁻³	-2.28 to +0.80 e Å ⁻³

Note: Graphite monochromatized Mo radiation; corrections for Lorentz and polarization effects; neutral-atomic complex scattering functions (Wilson 1992); program SHELXL-96 (Sheldrick 1996); $a = 31.62(1)$ Å, $Z = 16$ {Ca₄(K,Ca,Sr,Ba)₃Cu₃(Si,Al)₂₄O₄₈(OH)₈·xH₂O}, $x \geq 20$, Al:Si ~ 1:1, space group $Fm\bar{3}m$.

* Scan speed (2θ/ω-scan mode) = 0.45–0.90 °/min; scan width (+ α₁-α₂ dispersion) = 1.2°; background correction = 2 * 0.24°; 3 standards each 2 h; maximal variation of intensity is ±1.77%.

† Scan speed (φ-scan mode) = 0.16 °/min; Δφ = 1°/frame; frame size = binned mode, 621 × 576 pixels; detector-to-sample distance: 28 mm.

estimated to be approximately ±2 H₂O, based on a mean uncertainty of 2% regarding the individual constituents. The small amount of Fe is assumed to be Fe³⁺ substituting for Al and Si. On the basis of 48 framework O atoms the empirical formula is Ca_{5.60}Sr_{1.04}K_{0.70}Ba_{0.30}Cu_{2.90}Fe_{0.09}Al_{11.85}Si_{12.06}O₄₈(OH)_{8.44}·14.01H₂O. The simplified formula is Ca₄(K,Ca,Sr,Ba)₃Cu₃(OH)₈[Si₁₂Al₁₂O₄₈]·xH₂O. The essential components are supported by the results of the structure determination. Differences were obtained only for the sum of alkali and earth alkaline elements: 7.64 cations pfu were determined in the chemical analysis but only 7.00 atoms were localized at the Ca(1), Ca(2), and M position during the structure refinement. Further atomic positions suitable for these elements were not located in any of the cages. In addition, the structure refinement indicates for M = (K, Ca, Sr, Ba) an excess of atoms with higher atomic numbers such as Ba and Sr, whereas the analysis gave an excess of Ca and K. An atomic ratio Si:Al = 1:1 requires M²⁺; the incorporation of K¹⁺ for M probably will be balanced by an excess of Si. Variability of the chemical composition of individual tschörtnerite crystals could not be investigated due to lack of material, but the distinct zoning and the ranges of the microprobe results indicate that considerable chemical variability could exist. The water content derived from the structure investigation (approximately 20 H₂O molecules pfu) is larger than that calculated by difference from the electron-microprobe analysis (approximately 14 H₂O molecules pfu). The true water content should be higher; according to common experience the complete experimental location of the non-framework atoms in zeolites, and in particular of the water positions, is not achieved by X-ray structure investigation. The simplified formula as suggested by chemical analysis and structure investigation is Ca₄(K,Ca,Sr,Ba)₃Cu₃(OH)₈[Si₁₂Al₁₂O₄₈]·xH₂O, $x \geq 20$. The small amount of tschörtnerite available prohibited further analyses or investigation of dehydration and exchange mechanisms.

X-RAY STRUCTURE INVESTIGATION

For structure determination a small distorted cube was available, the edge lengths were only 0.04 × 0.06 × 0.08 mm. Initially, data collection was performed on a STOE AED2 diffractometer with a scintillation detector. The crystal volume was at the lower limit for conventional single-crystal X-ray diffraction and caused very weak X-ray reflections. This circumstance demanded extremely long measuring times. The cell parameter $a = 31.62(1)$ Å was obtained from 17 accurate 2θ angles, $V = 31614$ Å³, $Z = 16$. The absorption coefficient $\mu(\text{MoK}\alpha)$ is 27 cm⁻¹; due to this low value and due to the small size of the crystal an absorption correction was found to be negligible. Reflection conditions were characteristic for the space groups $F23$, $Fm\bar{3}$, $F432$, $F43m$, and $Fm\bar{3}m$; structure refinements prove the space group $Fm\bar{3}m$. The structure was solved by direct methods and subsequent Fourier and difference Fourier summations. The structure was refined with the program SHELXL-96 on F² (Sheldrick 1996), which allowed inclusion of the weak reflections in the refinement. The R-values were poor as it was expected from the small crystal size. Besides the tetrahedral framework, the cation positions Ca(1), Ca(2), M, Cu, and the hydroxyl O atoms, only the two atomic positions X and O_v(T2) within the cages could be located. Of course, it was impossible to derive crystal chemical details of the individual coordination polyhedra, nevertheless the correctness of the structure type was out of question.

A second data set was collected using a Nonius diffractometer equipped with a CCD detector. The new measuring technique allowed observations even at higher 2θ angles, the number of observed intensities with $F_o > 4\sigma(F_o)$ was increased from 383 to 1769. As a result, bond distances and bond angles became more accurate. Table 2 compiles the results of refinements from the two data sets. The average shift of the atom positions between the

TABLE 3. Structural parameters (e.s.d.'s in parentheses)

Atom	Site symmetry	Wyckoff letter	x	y	z	Occupation	U_{equiv} $U_{\text{isotropic}}$
Ca(1)	3m	32(f)	0.09965(5)	= x	= x	1.0	0.0259(6)
Ca(2)	3m	32(f)	0.20984(4)	= x	= x	1.0	0.0156(5)
(Ca,Sr,K,Ba) = M	m	96(j)	0.17945(4)	0.27909(4)	0	0.5	0.0340(5)
Cu	mm2	48(h)	0.07339(3)	= x	0	1.0	0.0293(4)
(Al,Si)(1) = T(1)	1	192(l)	0.10993(4)	0.18083(4)	0.24967(4)	1.0	0.0116(3)
(Al,Si)(2) = T(2)	1	192(l)	0.05044(4)	0.12239(4)	0.19243(4)	1.0	0.0120(3)
O _i (1)	1	192(l)	0.06740(11)	0.15559(9)	0.23003(10)	1.0	0.0191(7)
O _i (2)	m	96(k)	0.21169(10)	= x	0.13239(13)	1.0	0.0174(10)
O _i (3)	m	96(k)	0.21022(9)	= x	0.40798(13)	1.0	0.0167(10)
O _i (4)	m	96(k)	0.14640(10)	= x	0.26611(14)	1.0	0.0218(10)
O _i (5)	m	96(k)	0.14402(10)	= x	0.05687(16)	1.0	0.0263(11)
O _i (6)	m	96(k)	0.07720(11)	= x	0.19159(15)	1.0	0.0255(11)
O _i (7)	m	96(j)	0.11259(15)	0.20286(16)	0	1.0	0.0260(11)
O _n (1)	m	96(k)	0.04506(11)	= x	0.10539(11)	1.0	0.0274(11)
O _n (2)	3m	32(f)	0.28335(13)	= x	= x	1.0	0.0164(16)
X	m3m	4(a)	0	0	0	0.224(37)	0.011(12)
O _w (α1)	4mm	24(e)	0.041(3)	0	0	0.181(68)	0.068(49)
O _w (α2)	3m	32(f)	0.0262(10)	= x	= x	0.243(49)	0.050(22)
O _w (D6)	3m	32(f)	0.1467(4)	= x	= x	1.0	0.123(6)
O _w (8)	m	96(j)	0.0159(1)	0.1842(7)	0	0.305(18)	0.111(17)
O _w (D8)	m	96(j)	0.2087(3)	0.2339(3)	0	0.5	0.047(3)
O _w (T1)	1	192(l)	0.0085(19)	0.1316(9)	0.3048(10)	0.220(17)	0.132(18)
O _w (T2)	3m	32(f)	0.3599(2)	= x	= x	1.0	0.072(4)
O _w (T3)	m	96(k)	0.0336(11)	= x	0.2642(16)	0.195(17)	0.10*
O _w (T4)	1	192(l)	0.0714(11)	0.0888(12)	0.3105(10)	0.189(13)	0.10*
O _w (T5)	1	192(l)	0.0514(11)	0.1204(12)	0.3298(11)	0.400(34)	0.213(23)
Atom	U ₁₁	U ₂₂	U ₃₃	U ₂₃	U ₁₃	U ₁₂	
Ca(1)	0.0259(6)	= U ₁₁	= U ₁₁	0.0021(6)	= U ₂₃	= U ₂₃	
Ca(2)	0.0156(5)	= U ₁₁	= U ₁₁	-0.0011(5)	= U ₂₃	= U ₂₃	
M	0.0384(9)	0.0407(9)	0.0229(8)	0	0	-0.0110(6)	
Cu	0.0308(5)	= U ₁₁	0.0263(7)	0	0	-0.0013(5)	
T(1)	0.0119(6)	0.0117(6)	0.0112(6)	-0.0016(5)	-0.0008(5)	0.0005(5)	
T(2)	0.0101(6)	0.0119(6)	0.0141(7)	-0.0008(5)	-0.0016(5)	0.0007(5)	
O _i (1)	0.0174(17)	0.0212(17)	0.0188(17)	-0.0026(13)	0.0002(12)	-0.0022(13)	
O _i (2)	0.0200(15)	= U ₁₁	0.0123(22)	-0.0001(12)	= U ₂₃	-0.0002(18)	
O _i (3)	0.0164(15)	= U ₁₁	0.0174(23)	-0.0014(12)	= U ₂₃	0.0039(17)	
O _i (4)	0.0254(16)	= U ₁₁	0.0147(23)	0.0000(13)	= U ₂₃	0.0051(20)	
O _i (5)	0.0180(15)	= U ₁₁	0.0430(31)	-0.0017(14)	= U ₂₃	-0.0012(19)	
O _i (6)	0.0190(15)	= U ₁₁	0.0385(30)	-0.0046(15)	= U ₂₃	0.0064(19)	
O _i (7)	0.0310(28)	0.0366(29)	0.0105(23)	0	0	-0.0048(22)	
O _n (1)	0.0256(16)	= U ₁₁	0.0308(29)	-0.0005(15)	= U ₂₃	0.0022(21)	
O _n (2)	0.0164(16)	= U ₁₁	= U ₁₁	0.0002(18)	= U ₂₃	= U ₂₃	

Note: For the O_w atoms isotropic displacement parameters were refined. The anisotropic displacement parameter is defined as: $\exp[-2\pi^2 \sum_{i,j} \Sigma_{i,j}^2 U_{ij} a_i a_j h_i h_j]$, for U_{equiv} see Fischer and Tillmanns (1988).

* Fixed due to high correlation terms with the occupation factor.

two refinements is 0.028 Å, the maximum shift of a cation and an O atom was 0.03 and 0.07 Å, respectively. Several additional H₂O molecules were located during the refinement of the second data set, most of them are partially occupied. Some of the extra-framework O atoms revealed extremely high displacement parameters during refinement. These H₂O molecules are attached by weak hydrogen bonds to the framework; therefore they were not localized precisely, but show a (statical or dynamical) dislocation depending on the actual occupation of the individual sites in the neighborhood. For 2 O atoms the correlation terms between isotropic displacement parameter and site occupation factor were extremely high; therefore their U_{iso} was fixed during the final stage of structure investigation. Even during refinements of the second data set the allocation of the maximum X remained unclear. Slight discrepancies were maintained between analytical and structural data for the M position.

An uncertainty concerns the total water content; partially occupied atomic positions in addition to those included into the refinement are probable. The location of atoms at partially occupied positions is a well-known problem for natural and synthetic zeolites even for well-determined crystal structures. Further cations or even other small inorganic or organic molecules were not detected. Table 3 gives final atomic parameters for the refinements of the second data set.

Due to the small amount of material available for a powder diffraction sample, only very low counting rates could be observed. The quality of the observed XRD diagram was insufficient due to the poor intensities resulting from the structure; only the reflections at 18.3 Å (111) and at 15.8 Å (002) could be clearly observed. For a Debye-Scherrer diagram taken with a Gandolfi camera difficulties arise from the overlap of reflections caused by the large cell dimensions and the poor intensities. There-

TABLE 5. Cation positions

Bond lengths	(Å)	Multi- plicity*	Bond angle	(°)	Multi- plicity*
Ca(1)-O _i (5)	2.401(4)	3×	O _i (5)-Ca(1)-O _i (5)	108.5(1)	3×
Ca(1)-O _n (1)	2.448(4)	3×	O _i (5)-Ca(1)-O _n (1)	88.4(2)	6×
Ca(1)-O _i (6)	3.076(5)	3×	O _i (5)-Ca(1)-O _i (1)	150.0(2)	3×
Ca(1)-O _w (D6)	2.575(12)	1×	O _n (1)-Ca(1)-O _n (1)	66.9(1)	3×
			O _i (5)-Ca(1)-O _w (D6)	69.6(3)	3×
Ca(2)-O _i (2)	2.344(4)	3×	O _n (2)-Ca(2)-O _n (2)	79.0(2)	3×
Ca(2)-O _i (2)	2.450(4)	3×	O _i (2)-Ca(2)-O _i (2)	93.8(1)	6×
Ca(2)-O _i (4)	3.349(4)	3×	O _i (2)-Ca(2)-O _i (2)	170.6(2)	3×
			O _i (2)-Ca(2)-O _i (2)	92.7(1)	3×
M...M	1.854(2)	1×	O _i (-1)M-O _i (1)	102.0(1)	1×
M O _i (1)	2.742(3)	2×	O _i (-1)M-O _i (3)	54.3(1)	2×
M O _i (3)	3.087(4)	2×	O _i (-1)M-O _i (3)	151.8(1)	2×
M O _i (7)	3.206(5)	1×	O _i (-3)M-O _i (3)	141.0(1)	1×
M O _w (D8)	2.766(2)	1×	O _i (-1)M-O _i (7)	52.6(1)	2×
M O _w (D8)	2.813(9)	1×	O _i (-3)M-O _i (7)	106.9(1)	2×
M O _w (T1)	2.882(59)	2×			
M O _w (T5)	2.950(36)	2×			
CuO _n (1)	1.964(4)	4×	O _n (1)-CuO _n (1)	86.8(2)	2×
CuO _w (α2)	2.267(3)	2×	O _n (1)-CuO _n (1)	93.0(2)	2×
CuO _w (α1)	2.535(1)	2×	O _n (1)-CuO _n (1)	175.2(2)	2×
T(1)-O _i (4)	1.669(4)	1×	O _i (4)-T(1)-O _i (3)	111.1(2)	1×
T(1)-O _i (3)	1.671(4)	1×	O _i (4)-T(1)-O _i (2)	107.8(2)	1×
T(1)-O _i (1)	1.683(3)	1×	O _i (4)-T(1)-O _i (1)	111.0(2)	1×
T(1)-O _i (2)	1.703(4)	1×	O _i (3)-T(1)-O _i (2)	111.0(2)	1×
			O _i (3)-T(1)-O _i (1)	105.8(2)	1×
			O _i (2)-T(1)-O _i (1)	110.2(2)	1×
T(2)-O _i (7)	1.658(5)	1×	O _i (7)-T(2)-O _i (6)	109.4(2)	1×
T(2)-O _i (6)	1.661(4)	1×	O _i (7)-T(2)-O _i (1)	106.5(2)	1×
T(2)-O _i (1)	1.674(3)	1×	O _i (7)-T(2)-O _i (5)	111.8(2)	1×
T(2)-O _i (5)	1.689(5)	1×	O _i (6)-T(2)-O _i (1)	112.8(2)	1×
			O _i (6)-T(2)-O _i (5)	105.8(2)	1×
			O _i (1)-T(2)-O _i (5)	110.6(2)	1×
X...Cu	3.282(1)	12×	T(1)-O _i (1)-T(2)	144.6(2)	1×
X...O _w (α1)	1.30(9)	6×	T(1)-O _i (2)-T(2)	129.4(2)	1×
X...O _w (α2)	1.44(3)	8×	T(1)-O _i (3)-T(2)	136.8(2)	1×
			T(1)-O _i (4)-T(2)	143.6(3)	1×
			T(1)-O _i (5)-T(2)	136.0(2)	1×
			T(1)-O _i (6)-T(2)	151.2(2)	1×
			T(1)-O _i (7)-T(2)	148.3(3)	1×

* Partial occupations are not considered.

fore an X-ray powder pattern was calculated from the atomic parameters derived from single-crystal structure investigation for diffractometer geometry and CuK α radiation (see Appendix Table 4 and Appendix Fig. 3).

DESCRIPTION OF THE CRYSTAL STRUCTURE

Although tschörtnerite is a zeolite with a new structure type involving a new cage (Meier et al. 1996) and a new cluster formed by the extraframework Cu atoms, all individual coordination polyhedra are in agreement with known crystal chemical data. Bond lengths and bond angles are given in Table 5, bond valences in Table 6. O atoms belonging to the tetrahedral net, to hydroxyl groups, and to water molecules are denoted O_i, O_n, and O_w; the labels of the O_w atoms are relevant to their position within the individual cages.

The tetrahedral framework

The three-dimensional tetrahedral net with Si:Al 1:1 is formed by two crystallographically different (Al,Si)O₄ =

TABLE 6. Bond valences*

	Ca(1)	Ca(2)	Cu	T(1)	T(2)	Σ	Additional contribution
O _i (1)	—	—	—	0.88	0.90	1.78	M-O _i (1)
O _i (2)	—	0.27	—	0.84	—	1.95	—
O _i (3)	—	—	—	0.92	—	1.84	M-O _i (3)
O _i (4)	—	0.02	—	0.92	—	1.86	—
O _i (5)	0.31	—	—	—	0.87	2.05	—
O _i (6)	0.05	—	—	—	0.94	1.93	—
O _i (7)	—	—	—	—	0.95	1.90	M-O _i (7)
O _n (1)	0.27	—	0.46	—	—	1.19	—
O _n (2)	—	0.36	—	—	—	1.08	—
O _w (D6)	0.19	—	—	—	—	0.19	—
Σ	2.09	1.97	1.85	3.56	3.66		

Note: The contribution of the H atoms is neglected, for T a ratio Al:Si = 1:1 was assumed; due to the uncertainty of M these values are omitted. In valence units, see Brese and O'Keeffe 1991.

TO₄ tetrahedra that have site symmetry 1; only one out of the seven O_i atoms has site symmetry 1, the others are located at mirror planes. There is no evidence for a significant ordering of the Si and Al atoms within the two tetrahedral sites: the two average <T-O> bond lengths of 1.681 and 1.671 Å agree with an occupation Al:Si 1:1 (Smith and Bailey 1963; Jones 1968; Ribbe and Gibbs 1969). The variation of the individual T-O bond lengths from 1.658(5) to 1.703(4) Å and of the O-T-O bond angles from 105.8(2)° to 112.8(2)° in the two tetrahedra is in agreement with the variation generally found in silicates by Liebau (1985) and in zeolites (Gottardi and Galli 1985). The T-O(2)-T angle of 129.4(2)° is somewhat small and seems to be caused by the regular Ca(2)O₆ polyhedra inducing a slight strain to the framework. The other T-O-T angles that vary from 136.0(2)° to 151.2(2)° are energetically favorable.

The tetrahedral connection implies that Loewenstein's rule is not followed. Avoiding neighboring Al and Si tetrahedra requires the violation of the mirror planes and a reduction of space-group symmetry. However, the anisotropic displacement parameters gave no evidence for a splitting of any atoms of the tetrahedral net. The small number of observed reflections does not allow a substantial increase of refined parameters (even in the holohedral structure model the ratio of refined parameter to observations is only 1:13.7). Consequently a refinement of the structure model in any subgroup of *Fm* $\bar{3}$ *m* that might enable an ordering of the tetrahedral sites does not converge satisfactorily.

As characteristic for a zeolite, the tetrahedral framework consists of several cages (see Fig. 4 and Table 7): (1) the α -cage solely formed by the T(2)O₄ tetrahedra, (2) the β -cage solely formed by the T(1)O₄ tetrahedra, (3) the double eight ring (D8R), (4) the double six ring (D6R), and (5) the large super-cage (tschörtnerite-cage); (3) to (5) are formed half by T(1)O₄ and half by T(2)O₄ tetrahedra. The α - and β -cages house the Ca and Cu atoms as well as the hydroxyl groups; the O_n atom positions were found to be fully occupied. At the boundary between

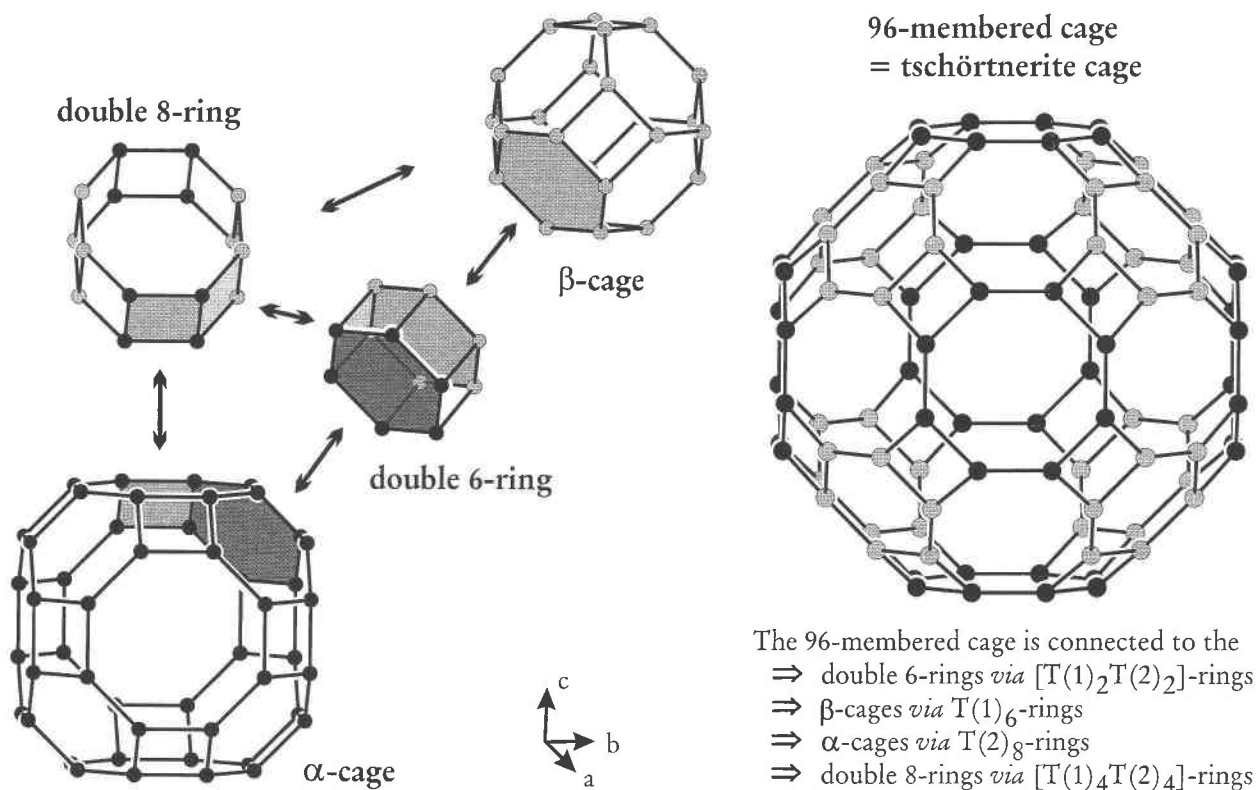


FIGURE 4. The five different cages in the tschörtnerite structure type and their connections. The T(1) atoms are light gray, the T(2) atoms are shown as dark gray balls. The T-O-T connection is represented by a straight line (program ATOMS, Dowty 1995).

D8R and tschörtnerite-cage are the M cations. Only water molecules are located within the D6R, the D8R, and the tschörtnerite-cages; the occupation with any further cations could not be verified.

The $\{Cu_{12}[O_h(1)_{24}]Ca(1)_8(O_l)_{24}(O_w)_8\}$ clusters within the α -cages

Most spectacular are $\{Cu_{12}[O_h(1)_{24}]Ca(1)_8(O_l)_{24}(O_w)_8\}$ clusters centered within the α -cages, they are depicted in

Figure 5a. The Cu atoms are square planar coordinated to hydroxyl groups with Cu- $O_h(1)$ bond lengths of 1.964(4) Å. This is one of the common coordination figures known for divalent Cu atoms. The site symmetry is $mm2$, the two mirror planes are perpendicular to the CuO_4 square. The 12 $Cu[O_h(1)]_4$ squares are corner-connected to a rhomb-dodecahedron-like complex with $m\bar{3}m$ symmetry in such a way that all corners of the $Cu[O_h(1)]_4$ squares link to two Cu atoms (Fig. 6a).

TABLE 7. The five cages within the crystal structure of tschörtnerite formed by the tetrahedral net

Description of the cage	Face symbol	Polyhedron	Center at positions	Observed symmetry	Highest attainable symmetry
Double 6-ring D6R, hexagonal prism	4^66^2	$[T(1)]_6[T(2)]_6$	$32(f)$ $(x\ x\ x)$, etc. $x = 0.1510$	$3m$	$6/mmm$
Truncated octahedron, β -cage sodalite cage	4^66^8	$[T(1)]_{24}$	$8(c)$ $(\frac{1}{4}\ \frac{1}{4}\ \frac{1}{4})$, etc.	$\bar{4}3m$	$m\bar{3}m$
Double 8-ring, δ -cage, D8R, octagonal prism	4^88^2	$[T(1)]_8[T(2)]_8$	$24(d)$ $(\frac{1}{4}\ \frac{1}{4}\ 0)$, etc.	mmm	$4/mmm$
Truncated cubo-octahedron, α -cage, great rhombicuboctahedron	$4^{12}6^88^6$	$[T(2)]_{48}$	$4(a)$ $(0\ 0\ 0)$, etc.	$m\bar{3}m$	$m\bar{3}m$
96-membered super-cage, tschörtnerite-cage, truncated great rhombicuboctahedron	$4^{24}6^88^68^{12}$	$[T(1)]_{48}[T(2)]_{48}$	$4(b)$ $(\frac{1}{2}\ \frac{1}{2}\ \frac{1}{2})$, etc.	$m\bar{3}m$	$m\bar{3}m$

Note: For face symbols cf. Smith (1989) and Meier et al. (1996) and references therein.

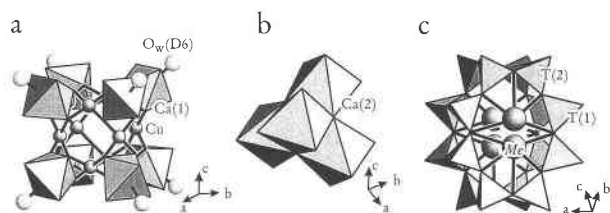


FIGURE 5. The coordination of the cations Ca, Cu, and M within the cages of tschörtnerite: (a) the $\{\text{Cu}_{12}[\text{O}_h(1)\text{H}]_{24}\} \text{Ca}(1)_8[\text{O}_i(5)]_{24}(\text{O}_w)_8$ cluster centered within the truncated cubo-octahedron with $m\bar{3}m$ symmetry, the bonds to the O_w atoms overlap to the D6R; (b) the $\text{Ca}(2)_4[\text{O}_h(2)]_4[\text{O}_i(2)]_{12}$ clusters within the sodalite cage with symmetry $43m$; (c) the half-occupied position of the (K,Ca,Sr,Ba) atoms within the top and bottom face of the D8R with mmm symmetry (program ATOMS, Dowty 1995). $Me = M$ in text.

The Ca(1) atom has the site symmetry $3m$ and is coordinated by seven ligands. Three ligands belong to the tetrahedral net, three are hydroxyl groups of the $\text{Cu}(\text{O}_h)_4$ squares; only slightly longer is the bonding distance to the fully occupied water-oxygen atom $\text{O}_w(\text{D6})$. The six nearest ligands form a distorted octahedron; the face formed by the O_i atoms is enlarged and capped by the $\text{O}_w(\text{D6})$ atom. The eight $\text{Ca}(1)\text{O}_7$ polyhedra are cube-like branched to the $\text{Cu}_{12}\text{O}_{24}$ unit, the $\text{Ca}(1)\text{O}_7$ polyhedron shares three edges with three CuO_4 squares (Fig. 6b).

Two partially occupied O atom positions $\text{O}_w(\alpha 1)$ and $\text{O}_w(\alpha 2)$ and an additional site with a still unclear allocation labeled X are encapsulated within this Cu cluster; additional interaction between the Cu atoms and one of these O_w atoms is evident. The Fourier peak named X was first refined with scattering factors of an O atom; an occupancy of 0.47(8) and negative values for U_{iso} were obtained. If real for an atomic position with a site multiplicity of 4/192, a partial occupation with an atom with a higher atomic number than O might be suggested; final refinements were performed arbitrarily with chlorine. The distances $\text{X}-\text{O}_w(\alpha 1)/\text{O}_w(\alpha 2)$ are 1.30(9) Å/1.44(3) Å, $\text{X}-\text{Cu} = 3.282(1)$ Å; X might be an anion like Cl, if the positions $\text{O}_w(\alpha 1)$ and $\text{O}_w(\alpha 2)$ are vacant within the special cage, or X might be a cation like S or even P: $\text{S}^{6+}/\text{P}^{5+}$ might be surrounded tetrahedrally by four $\text{O}_w(\alpha 2)$ atoms to form SO_4/PO_4 groups; consequently, in the latter case $\text{O}_w(\alpha 2)$ is to be interpreted only in parts as a water-oxygen atom. Jasmundite (Dent Glasser and Lee 1981) contains S^{2-} . It should be mentioned that X cannot accumulate parts of the Ca or K excess found in the electron-microprobe investigation. Due to the decomposition of tschörtnerite even in a defocused beam, the 0.05(2) wt% Cl found in the microprobe investigation can only be regarded as a hint.

The $\text{Ca}(2)_4[\text{O}_h(2)]_4[\text{O}_i(2)]_{12}$ clusters within the β -cages

Like the Ca(1) atom, the Ca(2) atom has site symmetry $3m$. It is fairly regular octahedrally coordinated by three ligands belonging to the tetrahedral net and by three hy-

droxyl groups. There is no interaction with further O_w atoms; consequently the $\text{Ca}(2)-\text{O}_i$ and $\text{Ca}(2)-\text{O}_h$ bond lengths are somewhat shorter than the $\text{Ca}(1)-\text{O}_i$ and $\text{Ca}(1)-\text{O}_h$ bonds. However, the average $\langle \text{Ca}(2)-\text{O} \rangle$ bond length is slightly larger than for the sixfold-coordinated Ca atom found in calcite (Effenberger et al. 1981). The $\text{Ca}(2)\text{O}_6$ octahedra are edge connected to each other. Four $\text{Ca}(2)\text{O}_6$ octahedra form $\text{Ca}_4[\text{O}_h(2)]_4[\text{O}_i(2)]_{12}$ clusters within the β -cages (Fig. 5b). The $\text{O}_i(2)$ atoms are bound to three Ca(2) atoms. The $\text{O}_h(2)$ and $\text{O}_i(2)$ atoms form a local cubic close-packed arrangement: four octahedral positions are occupied by the Ca(2) atoms, the central tetrahedral position is vacant.

The M = (K,Ca,Sr,Ba) atoms and the D8R

The M position is at most half occupied by K, Ca, Sr, and Ba atoms to avoid the M-M distances of only 1.87(2) Å, which is too short for a cation-cation contact. Such partially occupied cation positions have been often found in zeolites. The M atoms are located within the basal and top face of the D8R (Fig. 5c), i.e., the boundary toward the tschörtnerite cage. The eight-membered rings are elliptically distorted with T-T distances of 7.65 and 8.28 Å (cf. Bieniok and Bürgi 1994). The M atom is (statistically) shifted along the longer diameter of this ring to either side to fit the M-O bonds. The five ligands belonging to the tetrahedral net have M-O bond lengths between 2.742(3) to 3.206(5) Å; these ligands are arranged in an approximate plane. Up to four further H_2O molecules occupy positions at both sides of this plane to complete the coordination of the M atom (Fig. 6c). The M atom exhibits the largest anisotropic displacement parameters found for the non-water atoms in tschörtnerite, the principal mean-square atomic displacements are 0.051, 0.028, and 0.023 Å².

During refinement the ratio K/Ba was varied: The scattering power of K and Ca is similar, the Sr content was fixed to the analytically derived value of 1.03 atoms pfu. The sum of the site occupation factors was fixed to 0.5. The refinement yielded 0.65(4) K (and Ca) atoms pfu and 1.32 Ba atoms pfu. The discrepancy to the 0.30 Ba atoms pfu found analytically is large and might indicate a variation of the composition of tschörtnerite for individual samples.

The 96-membered cage (tschörtnerite cage)

The tschörtnerite cage consists of 50 faces formed by 6+12 eight-membered, 8 six-membered, and 24 four-membered rings. This polyhedron can be derived from the α -cage by adding a tetragon-trioctahedron. The faces of the crystallographic forms $\{100\}$, $\{111\}$, $\{110\}$, and $\{112\}$ are represented by the $\text{T}(2)_8$, $\text{T}(1)_6$, $\text{T}(1)_4\text{T}(2)_4$, and $\text{T}(1)_2\text{T}(2)_2$ rings, respectively. The new cage is best described by the term "truncated great rhombicuboctahedron." An occupation with at least five positions of H_2O molecules is proved by structure refinement (Fig. 6d). The tschörtnerite cage is the largest terminated cage known for zeolites. It has 96 corners, which is twice as

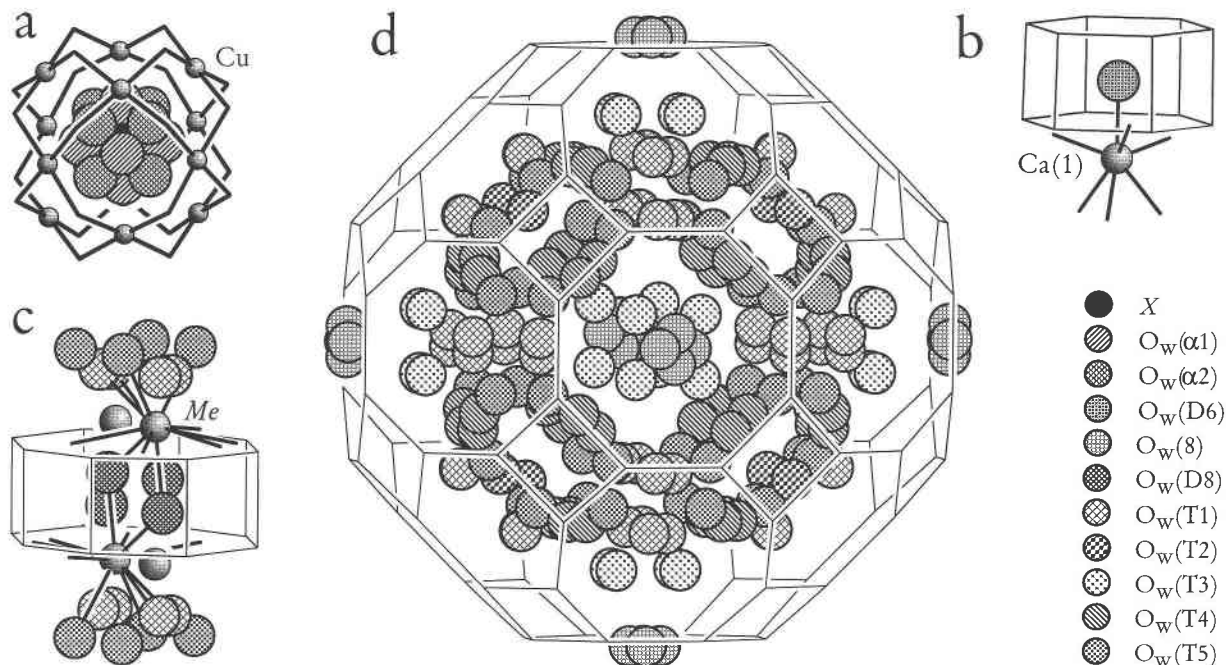


FIGURE 6. The H_2O molecules within the cages of tschörtnerite: (a) the $\text{O}_w(\alpha 1)$, $\text{O}_w(\alpha 2)$, and X position within the $\{\text{Cu}_{12}[\text{O}_8(1)\text{H}]_{24}\}$ cluster centered in the truncated cubo-octahebron; (b) the $\text{O}_w(\text{D}6)$ atom within the D6R completing the coordination of the Ca(1) atom; (c) the atoms $\text{O}_w(\text{D}8)$, $\text{O}_w(\text{T}1)$, and $\text{O}_w(\text{T}5)$ completing the coordination of the half-occupied atoms

$\text{M} = (\text{K}, \text{Ca}, \text{Sr}, \text{Ba})$ within the top and bottom face of the D8R; (d) the atoms $\text{O}_w(\text{T}1)$ to $\text{O}_w(\text{T}5)$ located within the tschörtnerite cage and the $\text{O}_w(8)$ atom within one of the two crystallographically different octagonal faces shared with the α -cage (program ATOMS, Dowty 1995). $\text{Me} = \text{M}$ in text.

much than in the α -cage. Large cages have been described, e.g., in the natural occurring zeolites chabazite (Smith et al. 1963), willhendersonite (Tillmanns et al. 1984), erionite (Kawahara and Curien 1969), levyne (Merlino et al. 1975), or gmelinite (Vezzalini et al. 1990). Another large unit is the double 40-ring of paulingite (Bienoik et al. 1996; Lengauer et al. 1994, 1997).

The double six-ring

The D6R is formed by six T(1) atoms forming the bottom and six T(2) atoms forming the top face. The $\text{O}_w(\text{D}6)$ atom is located within the center and is bound to the Ca(1) atom (Fig. 6b).

The H_2O molecules

The site symmetries $3m$ and $4mm$ found for parts of the O_w atoms are absolutely inconsistent with the $mm2$ symmetry of a water molecule. Therefore, a site disorder concerns at least the H atoms, but even a local disorder of the O_w atoms has to be assumed because of their high displacement parameters. Most of the H_2O molecules filling the pores of the cage system are highly disordered and only weakly bound to each other or to the framework atoms by hydrogen bonds; thus they could not be located precisely. Probable hydrogen bonds are compiled in Table 8.

REMARKS ON THE TYPE STRUCTURE

The unit cell contains 4 α -cages, 4 tschörtnerite cages, 8 β -cages, 24 D8R, and 32 D6R. Their connection is shown in Figures 7a and 7b in slices parallel to (100) and (110), respectively. Faces of the α -cages and β -cages are connected to each other by the basis and top face of the D6R and by the prismatic faces of the D8R. All these units are connected to the 96-membered cage. The complex type structure may be derived from the NaCl structure with the centers of the α - and tschörtnerite cages located at the Na and Cl positions, respectively. They are directly connected in [100] by eight-membered rings solely formed by the $\text{T}(2)\text{O}_4$ tetrahedra. Parallel to [110] the tschörtnerite cages are linked by the basal faces of the D8R; in addition parallel to [110] opposite prism faces of the D8R link to the α -cages [by four-membered rings formed by $\text{T}(2)\text{O}_4$ tetrahedra]. In [111] the sequence of interconnected cages is α -cage, D6R, β -cage, tschörtnerite cage, β -cage, D6R, and back to the α -cage (cf. Fig. 4). This connection scheme causes the reduction of the highest attainable symmetry of the β -cage $m\bar{3}m$ to $\bar{4}3m$, because the faces belonging to a tetrahedron (i.e., half of the "octahedral" faces) are shared with the D6R, and faces of the other tetrahedron are shared with the tschörtnerite cage. The tetrahedral net found in tschörtnerite was unknown for both natural and synthetic zeolites; Smith

TABLE 8. Probable hydrogen bonds of the hydroxyl groups and H₂O molecules in tschörtnerite

O _h (1)···O _w (8)	3.02(2)	O _w (D6)···O _i (2)	2.943(12)	O _w (T1)···O _w (T1)	2.85(8)
O _h (1)···O _i (6)	3.081(6)	O _w (8)···O _i (7)	3.11(3)	O _w (T1)···O _w (T1)	2.90(8)
O _h (2)···O _i (4)	3.188(6)	O _w (D8)···O _i (1)	2.717(7)	O _w (T1)···O _w (T4)	3.18(7)
		O _w (D8)···O _i (7)	3.195(12)	O _w (T1)···O _w (T4)	2.87(7)
O _w (α1)···O _w (α1)	2.60(13)	O _w (T1)···O _i (1)	3.10(6)	O _w (T1)···O _w (T5)	2.99(7)
O _w (α2)···O _w (α2)	2.87(4)	O _w (T1)···O _i (7)	3.29(6)	O _w (T1)···O _w (T5)	3.27(7)
O _w (8)···O _w (T3)	2.80(4)	O _w (T2)···O _i (4)	2.980(8)	O _w (T2)···O _w (T4)	3.13(3)
O _w (8)···O _w (T3)	3.16(4)	O _w (T3)···O _i (6)	3.01(3)	O _w (T2)···O _w (T5)	3.03(4)
O _w (D8)···O _w (D8)	2.564(15)	O _w (T3)···O _i (7)	3.34(3)	O _w (T3)···O _w (T3)	3.01(5)
		O _w (T4)···O _i (1)	3.31(3)	O _w (T3)···O _w (T4)	2.57(5)
		O _w (T4)···O _i (4)	3.30(4)	O _w (T5)···O _w (T5)	3.08(5)
		O _w (T5)···O _i (1)	3.38(4)	O _w (T5)···O _w (T5)	3.25(5)
		O _w (T5)···O _i (3)	3.36(4)		

Note: Bond lengths with $2.50 \text{ \AA} \leq \text{O} \cdots \text{O} \leq 3.40 \text{ \AA}$ are given. O···O contacts representing an edge in coordination polyhedra of Ca(1), Ca(2), M, or Cu are excluded.

and Bennett (1981) discussed the net based on theoretical considerations.

The tetrahedral framework of tschörtnerite is very loose packed as compared with common experience. According to Meier et al. (1996) the framework density is

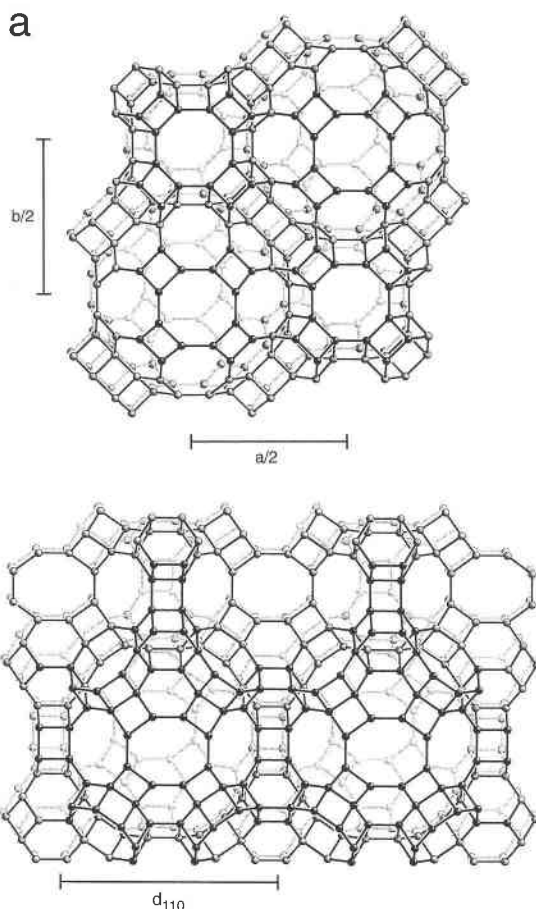


FIGURE 7. Slices of the tetrahedral net in tschörtnerite. (a) The connection of the α - and tschörtnerite cages with the D8R in (100), some of the D6R are branched. (b) The connection of the α - β -, and tschörtnerite cages with the D8R in (110), some of the D6R are branched.

the lowest known for a zeolite and amounts 12.15 tetrahedra per 1000 \AA^3 . Framework densities between 12.5 and 13.0 are known for the natural zeolite faujasite and its isotypic framework structures and compositional and hexagonal structure variants (Baur 1964) as well as for the zeolites CoAPO-50 (Akolekar 1995) and Linde Type A (Gramlich and Meier 1971). A lower density was described for the interrupted framework of cloverite (Estermann et al. 1991).

Tschörtnerite is a zeolite with an extremely large cage, but the largest pore openings are only single and double eight-rings. Therefore the exchange mechanisms are expected to be moderate. The densely filled α - and β -cages seem to be an obstacle for exchange reactions and hydration and dehydration processes. The most probable path for exchange reactions seems to be by the basal faces of the D8R and the tschörtnerite-cages.

Some natural and synthetic zeolites are known to form unit cells that are among the largest known for inorganic compounds. Zeolites with a larger unit cell as compared with tschörtnerite are paulingite (Bienoik et al. 1996; Lengauer et al. 1994, 1997), NaZ-21 (Shepelev et al. 1983), and N (Fälth and Andersson 1982). In the title compound the large cell is a consequence of the huge tschörtnerite cage.

All natural zeolites that have been described up to now are nominally copper-free. Due to their catalytic properties, multiple exchange reactions and their mechanisms were described for zeolites. Among many others they concern the minerals faujasite (Maxwell and Boer 1975), chabasite (Pluth et al. 1977), pollucite, and the synthetic zeolites Y (Gallezot et al. 1972; Martí et al. 1976; Kaushik and Ravindranathan 1992), NaCuY (Martí et al. 1976), A (Lee and Seff 1981; Moretti 1994), SAPO-5 and SAPO-11 (Lee and Seff 1981), NaX (Vlissidis et al. 1993), or Cu-ZSM-5 (Kucherov et al. 1995a, 1995b, see also references therein) For more information about Cu atoms on framework sites in zeolites see Heinrich and Baerlocher (1991).

ACKNOWLEDGMENTS

We thank J. Tschörtner and G. Tremmel for supplying material for investigation, G. Röller, Ruhr-Universität Bochum, for the Fourier-transform

IR measurements, and O. Medenbach, Ruhr-Universität Bochum, for the determination of the refractive index. Helpful comments by A. Alberti, G. Artioli, and J.V. Smith improved the manuscript.

REFERENCES CITED

- Abraham, K., Gebert, W., Medenbach, O., Schreyer, W., and Hentschel, G. (1983) Eifelite, $\text{KNa}_2\text{Mg}_6\text{Si}_{12}\text{O}_{30}$, a new mineral of the osumilite group with octahedral sodium. *Contribution to Mineralogy and Petrology*, 82, 252–258.
- Akolekar, D.B. (1995) Novel, crystalline, large-pore magnesium aluminophosphate molecular sieve of type 50: preparation, characterization, and structural stability. *Zeolites*, 15, 583–590.
- Baur, W.H. (1964) On the cation and water positions in faujasite. *American Mineralogist*, 49, 697–704.
- Bieniok, A. and Bürgi, H.B. (1994) Deformation analysis of the D8R-unit in zeolite structures. *Studies Surface Science and Catalysis. Zeolites and related microporous materials: state of the art 1994*, Elsevier Science B.V., Amsterdam 84A, 567–574.
- Bieniok, A., Joswig, W., and Baur, W.H. (1996) A study of paulingites: pore filling by cations and water molecules. *Neues Jahrbuch für Mineralogie, Abhandlungen*, 171, 119–134.
- Brese, N.E. and O'Keeffe, M. (1991) Bond-valence parameters for solids. *Acta Crystallographica*, B47, 192–197.
- Colville, A.A. and Geller, S. (1971) The crystal structure of brownmillerite, $\text{Ca}_2\text{FeAlO}_5$. *Acta Crystallographica*, B27, 2311–2315.
- Colville, A.A. and Geller, S. (1972) Crystal structures of $\text{Ca}_2\text{Fe}_{1-43}\text{Al}_{0.57}\text{O}_5$ and $\text{Ca}_2\text{Fe}_{1-28}\text{Al}_{0.72}\text{O}_5$. *Acta Crystallographica*, B28, 3196–3200.
- Dent Glasser, L.S. and Lee, C.K. (1981) The structure of jasmundite, $\text{Ca}_{22}(\text{SiO}_4)_8\text{O}_4\text{S}_2$. *Acta Crystallographica*, B37, 803–806.
- Dowty, E. (1995) ATOMS 3.2. A Computer Program for Displaying Atomic Structures, Kingsport, TN 37663.
- Effenberger, H., Mereiter, K., and Zemann, J. (1981) Crystal structure refinements of magnesite, calcite, rhodochrosite, siderite, smithsonite, and dolomite, with discussion of some aspects of the stereochemistry of calcite type carbonates. *Zeitschrift für Kristallographie*, 156, 233–243.
- Estermann, M., McCusker, L.B., Baerlocher, C., Merrouche, A., and Kessler, H. (1991) A synthetic gallophosphate molecular sieve with a 20-tetrahedral-atom pore opening. *Nature*, 352, 320–323.
- Fälth, L. and Andersson, S. (1982) Crystal structure of the synthetic zeolite N, $\text{NaAlSiO}_4 \cdot 1.35\text{H}_2\text{O}$. *Zeitschrift für Kristallographie*, 160, 313–316.
- Fischer, R.X. and Tillmanns, E. (1988) The equivalent isotropic displacement factor. *Acta Crystallographica*, C44, 775–776.
- Fischer, R.X., Lengauer, C.L., Tillmanns, E., Ensink, R.J., Reiss, C.A., and Fantner, E.J. (1993) PC-Rietveld plus, a comprehensive Rietveld analysis package for PC. *Materials Science Forum*, 133–136, 287–292.
- Frechen, J. (1971) Siebengebirge am Rhein, Laacher Vulkangebiet, Maargebirge der Westeifel. *Sammlung Geologischer Führer* no. 56, 209 p. Gebrüder Bornträger.
- Gallezot, P., Ben Taarit, Y., and Imelik, B. (1972) X-ray diffraction study of cupric ion migrations in two Y-type zeolites containing absorbed reagents. *Journal of Catalysis*, 26, 295–302.
- Gottardi, G. and Galli, E. (1985) Natural zeolites. In P.J. Wyllie, Ed., *Minerals and Rocks*, p. 409. Springer-Verlag, Berlin.
- Gramlich, V. and Meier, W.M. (1971) The crystal structure of hydrated NaA: a detailed refinement of a pseudosymmetric zeolite structure. *Zeitschrift für Kristallographie*, 133, 134–149.
- Hamm, H.M. and Hentschel, G. (1983) Reinhardbraunsite, $\text{Ca}_5(\text{SiO}_4)_2(\text{OH},\text{F})_2$, a new mineral—the natural equivalent of synthetic “calcio-chondrodite”. *Neues Jahrbuch für Mineralogie Monatshefte*, 119–129.
- Heinrich, A.R. and Baerlocher, C. (1991) X-ray Rietveld structure determination of $\text{Cs}_2\text{CuSi}_5\text{O}_{12}$, a pollucite analogue. *Acta Crystallographica*, C47, 237–241.
- Hentschel, G. (1964) Mayenit, $12\text{CaO} \cdot 7\text{Al}_2\text{O}_3$, und Brownmillerit, $2\text{CaO} \cdot (\text{Al},\text{Fe})_2\text{O}_3$, zwei neue Minerale in den Kalksteineinschlüssen der Lava des Ettringer Bellerberges. *Neues Jahrbuch für Mineralogie Monatshefte*, 22–29.
- Hentschel, G. (1987) *Die Mineralien der Eifelvulkane*, 2nd ed., 175 pages, Christian Weise Verlag.
- Hentschel, G. and Kuzel, H.J. (1976) Strätlingit, $2\text{CaO} \cdot \text{Al}_2\text{O}_3 \cdot \text{SiO}_2 \cdot 8\text{H}_2\text{O}$, ein neues Mineral. *Neues Jahrbuch für Mineralogie Monatshefte*, 326–330.
- Hentschel, G., Dent Glasser, L.S., and Lee, C.K. (1983) Jasmundite, $\text{Ca}_{22}(\text{SiO}_4)_8\text{O}_4\text{S}_2$, a new mineral. *Neues Jahrbuch für Mineralogie Monatshefte*, 337–342.
- Jones, J.B. (1968) Al-O and Si-O tetrahedral distances in aluminosilicate framework structures. *Acta Crystallographica*, B24, 355–358.
- Kaushik, V.K. and Ravindranathan, M. (1992) X.P.S. study of copper-containing Y zeolites for the hydration of acrylonitrile to acrylamide. *Zeolites*, 12, 415–419.
- Kawahara, A. and Curien, H. (1969) La structure cristalline de l'érieronite. *Bulletin de la Société française de Minéralogie et de Cristallographie*, 92, 250–256.
- Krause, W., Bernhardt, H.-J., Effenberger, H., and Giester, G. (1997) Tschörtnerite, a copper-bearing zeolite from the Bellberg volcano, Eifel, Germany. Abstracts of the 75th annual meeting of the Deutsche Mineralogische Gesellschaft, Cologne, September 15–19, 1997, *European Journal of Mineralogy*, 9, Beiheft 1, 209.
- Kucherov, A.V., Gerlock, J.L., Jen, H.-W., and Shelef, M. (1995a) *In situ* e.s.r. monitoring of the coordination and oxidation states of copper in Cu-ZSM-5 up to 500° in flowing gas mixtures: 1. Interaction with H_2 , O_2 , NO_2 , and H_2O . *Zeolites*, 15, 9–14.
- Kucherov, A.V., Gerlock, J.L., Jen, H.-W., and Shelef, M. (1995b) *In situ* e.s.r. monitoring of the coordination and oxidation states of copper in Cu-ZSM-5 up to 500° in flowing gas mixtures: 2. Interactions with CH_4 and CO . *Zeolites*, 15, 15–20.
- Lee, C.W. and Kevan, L. (1994) The comparative reactivity of various organic absorbates with Cu(II) in CuH-SAPO-5 and CuH-SAPO-11 molecular sieves studied by electron spin resonance. *Zeolites*, 14, 267–271.
- Lee, H.S. and Seff, K. (1981) Redox reactions of copper in zeolite A. Four crystal structures of vacuum-desolvated copper-exchanged zeolite A, $\text{Cu}_x\text{-A}$. *Journal of Physical Chemistry*, 85, 397–405.
- Lehmann, J. (1874) über den Ettringit, ein neues Mineral, in Kalksteineinschlüssen der Lava von Ettringen (Laacher Gebiet). *Neues Jahrbuch für Mineralogie, Geologie und Paläontologie*, 273–275.
- Lengauer, C.L., Giester, G., and Tillmanns, E. (1994) Paulingite, a new occurrence from Vinarická Hora, CSFR. Abstracts of the 16th General Meeting of the International Mineralogical Association, Pisa, 238.
- Lengauer, C.L., Giester, G., and Tillmanns, E. (1997) Mineralogical characterization of paulingite from Vinarická Hora, Czech Republic. *Mineralogical Magazine*, 61, 591–606.
- Liebau, F. (1985) *Structural chemistry of silicates. Structure, bonding and classification*, 347 p. Springer-Verlag, Berlin.
- Macleod, G. and Hall, A.J. (1991) Whisker crystals of the mineral ettringite. *Mineralogy and Petrology*, 43, 211–215.
- Martí, J., Soria, J., and Cano, F.H. (1976) Location of the cations in hydrated NaCuY zeolite. *Journal of Physical Chemistry*, 80, 1776–1780.
- Maxwell, I.E. and de Boer, J.J. (1975) Crystal structures of hydrated and dehydrated divalent-copper-exchanged faujasite. *Journal of Physical Chemistry*, 79, 1874–1879.
- Meier, W.M., Olson, D.H., and Baerlocher, C. (1996) *Atlas of zeolite structure types. Zeolites*, 17, 1–230.
- Merlino, S., Galli, E., and Alberti, A. (1975) The crystal structure of levynite. *Tschermaks Mineralogische und Petrographische Mitteilungen*, 22, 117–129.
- Moretti, G. (1994) The contribution of X-ray photoelectron and X-ray excited Auger spectroscopies in the characterization of zeolites and of metal clusters entrapped in zeolites. *Zeolites*, 14, 469–475.
- Pluth, J.J., Smith, J.V., and Mortier, W.J. (1977) Positions of cations and molecules in zeolites with the chabazite framework. IV Hydrated and dehydrated Cu^{2+} -exchanged chabazite. *Materials Research Bulletin*, 12, 1001–1007.
- Ribbe, P.H. and Gibbs, G.V. (1969) Statistical analysis and discussion of mean Al/Si O bond distances and the aluminum content of tetrahedra in feldspars. *American Mineralogist*, 54, 85–94.
- Rinaldi, R., Sacerdoti, M., and Passaglia, E. (1990) Strätlingite: crystal

- structure, chemistry, and a reexamination of its polytype vertumnite. *European Journal of Mineralogy*, 2, 841–849.
- Rüdinger, B., Tillmanns, E., and Hentschel, G. (1993) Bellbergite—a new mineral with the zeolite structure type EAB. *Mineralogy and Petrology*, 48, 147–152.
- Schüller, W. (1990) Die Mineralien des Bellerberges. *Lapis*, 15(5), 9–35.
- Sheldrick, G.M. (1996) SHELXL-96. Programs for Crystal Structure Determination, University of Cambridge, England.
- Shepelev, Y.F., Smolin, Y.I., Butikova, I.K., and Tarasov, V.I. (1983) The crystal structure of zeolite NaZ-21 in hydrated and dehydrated states. *Doklady Akademii Nauk SSSR*, 272, 1133–1137.
- Smith, J.V. (1989) Towards a comprehensive mathematical theory for the topology and geometry of microporous materials. *Studies Surface Science and Catalysis. Zeolites: Facts, Figures and Future*, Elsevier, Amsterdam, 49A, 29–47.
- Smith, J.V. and Bailey, S.W. (1963) Second review of Al-O and Si-O tetrahedral distances. *Acta Crystallographica*, 16, 801–811.
- Smith, J.V. and Bennett, J.M. (1981) Enumeration of 4-connected 3-dimensional nets and classification of framework silicates: the infinite set of ABC-6 nets; the Archimedean and σ -related nets. *American Mineralogist*, 66, 777–788.
- Smith, J.V., Rinaldi, F., and Dent Glasser, L.S. (1963) Crystal structure with a chabazite framework. II. Hydrated Ca-chabazite at room temperature. *Acta Crystallographica*, 16, 45–53.
- Treacy, M.M., Higgins, J.B., and von Ballmoos, R. (1996) Collection of simulated XRD powder patterns for zeolites. *Zeolites*, 16, 323–802.
- Tillmanns, E., Fischer, R.X., and Baur, W.H. (1984) Chabazite-type framework in the new zeolite willhendersonite, $KCaAl_3Si_3O_{12} \cdot 5H_2O$. *Neues Jahrbuch für Mineralogie Monatshefte*, 547–558.
- Vezzalini, G., Quartieri, S., and Passaglia, E. (1990) Crystal structure of a K-rich natural gmelinite and comparison with the other refined gmelinite samples. *Neues Jahrbuch für Mineralogie Monatshefte*, 504–516.
- Vlissidis, A.G., Evmiridis, N.P., Beagley, B., and Armitage, D.N. (1993) Cuprammine ion-exchanged NaX zeolite and crystal structure analysis. *Zeitschrift für Kristallographie*, 203, 17–27.
- Wilson, A.J.C., Ed. (1992) *International tables for crystallography*. Vol. C, mathematical, physical and chemical tables, 883 p. Kluwer, Dordrecht.

MANUSCRIPT RECEIVED JULY 14, 1997

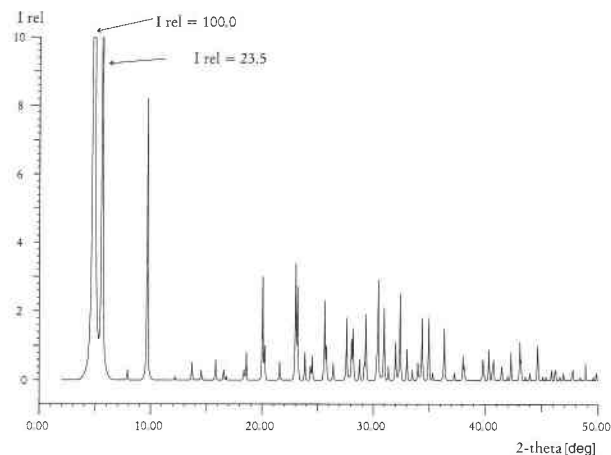
MANUSCRIPT ACCEPTED DECEMBER 1, 1997

PAPER HANDLED BY GILBERTO ARTIOLI

APPENDIX TABLE 4. Simulated XRD powder pattern of tschöртnerite

2 θ	d	I(rel)	hkl	2 θ	d	I(rel)	hkl
4.84	18.256	100.0	111	29.33	3.043	1.0	2 210
5.59	15.810	23.5	002	29.33	3.043	0.9	6 6 6
9.68	9.128	7.7	222	30.42	2.936	1.9	0 410
13.71	6.454	0.6	224	30.42	2.936	0.8	4 6 8
15.84	5.590	0.6	044	30.96	2.887	2.0	2 410
18.60	4.767	0.8	226	32.00	2.795	1.1	0 8 8
20.04	4.428	1.4	117	32.38	2.763	0.6	1 311
20.04	4.428	1.5	155	32.38	2.763	0.7	1 7 9
20.24	4.385	0.9	046	32.38	2.763	1.1	5 5 9
21.57	4.117	0.5	355	33.01	2.711	0.9	0 610
23.00	3.863	3.1	337	34.00	2.635	0.5	4 8 8
23.18	3.835	1.6	028	34.36	2.608	0.6	1 511
23.18	3.835	0.8	446	34.36	2.608	1.2	7 7 7
23.86	3.727	0.8	066	34.96	2.565	1.8	4 610
24.52	3.627	0.7	266	36.36	2.469	0.6	2 412
25.65	3.471	2.1	357	36.36	2.469	0.7	6 8 8
25.80	3.450	0.8	248	39.78	2.264	0.6	5 711
26.42	3.371	0.5	466	40.30	2.236	0.7	01010
27.62	3.227	1.7	448	43.07	2.099	0.7	5 911
28.06	3.178	0.6	339	44.64	2.028	0.6	9 9 9
28.20	3.162	0.6	0010	48.84	1.863	0.5	01212
28.20	3.162	0.8	068	53.30	1.717	0.6	11313
28.77	3.101	0.6	268	57.67	1.597	1.0	01414

Note: Diffractometer geometry, $CuK\alpha$ radiation (program "PC-Rietveld plus," Fischer et al. 1993; for standardization cf. Treacy et al. 1996).



APPENDIX FIGURE 3. Simulated XRD powder pattern of tschöртnerite for diffractometer geometry and $CuK\alpha$ radiation (program package PC-Rietveld plus, Fischer et al. 1993; for standardization cf. Treacy et al. 1996).